

^{13}C NMR Investigation of the Superconductor MgCNi_3 up to 800 K

P. M. Singer,¹ T. Imai,¹ T. He,² M. A. Hayward,² and R. J. Cava²

¹*Department of Physics and Center for Materials Science and Engineering, Massachusetts Institute of Technology, Cambridge, Massachusetts 02139*

²*Department of Chemistry and Princeton Materials Institute, Princeton University, Princeton, New Jersey 08544*
(Received 22 June 2001; published 30 November 2001)

We report ^{13}C NMR characterization of the new superconductor MgCNi_3 [T. He *et al.*, Nature (London) **411**, 54 (2001)]. We found that both the uniform spin susceptibility and the spin fluctuations show a strong enhancement with decreasing temperature, and saturate below ~ 50 K and ~ 20 K, respectively. The nuclear spin-lattice relaxation rate $1/^{13}\text{T}_1$ exhibits typical behavior for isotropic *s*-wave superconductivity with a coherence peak below $T_c = 7.0$ K that grows with decreasing magnetic field.

DOI: 10.1103/PhysRevLett.87.257601

PACS numbers: 76.60.-k, 74.20.Mn, 74.25.-q

Over the past several years, two new major trends have emerged in the research on superconductivity. One is the search for superconducting ground states near magnetic instabilities. Mathur *et al.*, for example, have demonstrated that application of high pressure transforms the antiferromagnetic ground states of some heavy Fermion materials into superconductors [1]. The exotic superconductor Sr_2RuO_4 [2,3] exhibits more subtle signatures of magnetic correlations in the normal state above T_c [4,5]. Another emerging trend is the search for superconductivity in intermetallic compounds with light elements. Recently, Nagamatsu *et al.* discovered superconductivity in MgB_2 [6]. High frequency phonons induced by the light element, B, are believed to be essential in yielding the high T_c .

A very recent addition to the list of new superconductors along these trends is MgCNi_3 [7–12]. MgCNi_3 forms a three-dimensional perovskite structure. Mg, C, and Ni replace Sr, Ti, and O in SrTiO_3 , respectively. Six Ni atoms at the face-centered position of each cubic unit cell form a three-dimensional network of Ni_6 -octahedra. Each C atom is located in the body-centered position surrounded by a Ni_6 -octahedron cage. Ni *3d* orbitals and C *2p* orbitals form two electronic bands at the Fermi level, one being electronlike and the other holelike [13–16]. The superconducting transition temperature is modestly high, $T_c = 7.0$ K, for an intermetallic system. The discovery of a superconducting ground state in MgCNi_3 poses two interesting questions: First, what is the role played by Ni *3d* electrons? Unfilled Ni *3d* orbitals usually form magnetically correlated bands, and recent band calculations indicate predominantly Ni *3d* character at the Fermi level [13–16]. Furthermore, if C atoms are removed from MgCNi_3 , MgNi_3 is expected to have a magnetic ground state [14]. These calculations imply that MgCNi_3 may also be on the verge of a magnetic instability. Unfortunately, the volatility of Mg in chemical reaction processes [7] makes growth of bulk samples difficult, and no details of possible electronic correlation effects have been addressed by conventional bulk measurement techniques. Second, does the presence of C, a light element, imply that the phonon-mediated BCS mechanism is at work for

stabilizing the superconducting ground state? Recent tunneling measurements by Mao *et al.* detected a zero bias conductance peak below T_c [11], suggesting otherwise. The tunneling result may be interpreted as an indication of the unconventional character of the superconducting pairing state.

In this Letter, we report the first ^{13}C NMR investigation of MgCNi_3 both above and below T_c . Our sample was prepared in a manner similar to that previously reported [7], but with ^{13}C enriched graphite as the starting material to enhance the intensity of the ^{13}C NMR signal. This allowed us to follow the temperature dependence of the ^{13}C NMR properties in a broad temperature range between 1.7 and 800 K. We demonstrate that the normal state properties of MgCNi_3 show the signature of modest electronic correlation effects. Both the uniform spin susceptibility $\chi'(q=0)$, as measured by the Knight shift ^{13}K , and the spin fluctuations, as measured by the nuclear spin-lattice relaxation rate $1/^{13}\text{T}_1$ divided by temperature T ($1/^{13}\text{T}_1T$), increase monotonically below 800 K down to ~ 50 K and ~ 20 K, respectively, before saturating to a constant value. A single *Korringa relation* for a Fermi liquid $1/T_1TK^2 = \text{const}$, *cannot* account for the temperature dependences of ^{13}K and $1/^{13}\text{T}_1T$ between 800 K and T_c . The most likely scenario is that electronic correlation effects enhance both the static and the dynamic magnetic susceptibility, and a modestly mass-enhanced Fermi-liquidlike state is realized somewhat above T_c . Overall, the normal state NMR properties of MgCNi_3 bear significant qualitative similarities with those of the exotic superconductor Sr_2RuO_4 . However, we demonstrate that our NMR data below T_c are consistent with conventional *s*-wave pairing.

In Fig. 1(a), we present the Fourier transformed ^{13}C NMR line shape from MgCNi_3 powder. Above T_c , ^{13}C in MgCNi_3 has a large, temperature-dependent, positive NMR Knight shift ^{13}K with much narrower linewidth than the overall NMR shift. The narrow linewidth above T_c is consistent with the fact that the carbon site has cubic point symmetry which ensures the absence of any shift anisotropy.

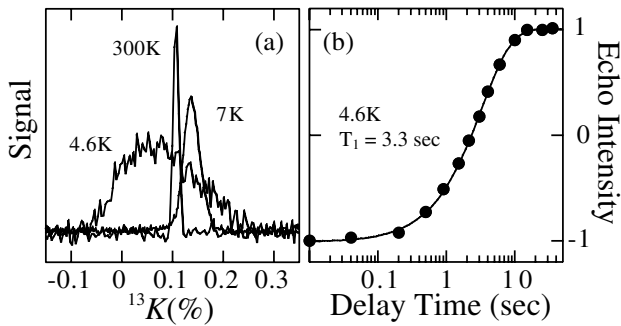


FIG. 1. (a) A Fourier transformed ^{13}C NMR spectrum (arbitrary units) in MgCNi_3 obtained at 4.6, 7, and 300 K in 1 T. (b) A typical ^{13}C NMR spin echo recovery at 4.6 K and 1 T. A 180° saturation pulse was employed. The solid line is the best fit to a single exponential recovery with $T_1 = 3.3$ sec.

In Fig. 2(a), we present the temperature dependence of the powder averaged NMR Knight shift ^{13}K . According to band calculations [13–16], MgCNi_3 has two bands arising from Ni $3d$ and C $2p$ hybridization at the Fermi energy. In terms of the spin susceptibility $\chi_j'(q=0)$ of the j th band ($j = 1, 2$ is the band index), one can write ^{13}K as [17]

$$^{13}K = \sum_j A_j \chi_j'(q=0) + ^{13}K_{\text{orb}}. \quad (1)$$

where A_j is the hyperfine coupling constant between the ^{13}C nuclear spin ($I = \frac{1}{2}$) and the electrons in the j th band. $^{13}K_{\text{orb}}$ is the orbital contribution in the nearly filled $2p$ orbitals of the C atoms, and in various materials such as graphite, it is known to be as small as 0.01%–0.02%. $A_j \chi_j'(q=0)$ represents the spin contribution to the Knight shift from the j th band. Since the hyperfine interaction is dominated by s electrons, it is safe to assume that $A_1 \sim A_2$. Accordingly, the results in Fig. 2(a) suggest that the total spin susceptibility $\sum_j \chi_j'(q=0)$ increases by approximately 50%–70% below 800 K down to T_c , if we take

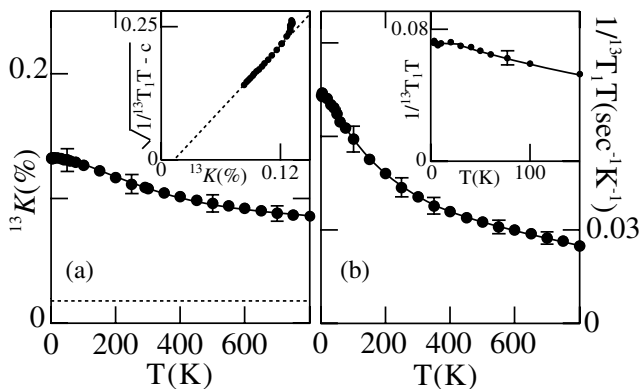


FIG. 2. (a) Temperature dependence of the ^{13}C NMR Knight shift ^{13}K . The solid curve is a guide for the eyes and the dashed line is $^{13}K = 0.018\%$ for graphite. Inset of (a): $\sqrt{1/^{13}T_1T - c}$ vs ^{13}K . The dashed line above 120 K is with $c = 0.005$ sec K^{-1} and $\beta = 6.0$ (see text). (b) Temperature dependence of $1/^{13}T_1T$ measured in 9 T. The solid curve is a guide for the eyes. Inset of (b): $1/^{13}T_1T$ below 150 K.

$^{13}K_{\text{orb}} = 0.01\% - 0.02\%$. Needless to say, we cannot rule out the possibility that $\chi_1'(q=0)$ and $\chi_2'(q=0)$ exhibit somewhat different temperature dependences. The temperature dependence of ^{13}K changes curvature at about $T^* \sim 50$ K. The electrical resistivity data also show a change of curvature in the same temperature range, and satisfy $\rho \sim T^n$ with $n \sim 1.8$ below $T^* \sim 50$ K [18]. These results suggest that an electronic crossover takes place near $T^* \sim 50$ K prior to the superconducting transition at $T_c = 7.0$ K.

From standard $K - \chi$ analysis [17], where we choose $^{13}K_{\text{orb}} = 0.014\%$ from the inset of Fig. 2(a), we obtained $A_1 = A_2 \sim 14$ kOe/ μ_B , the sum of the diamagnetic and Van Vleck contribution as $\chi_{\text{dia}} + \chi_{\text{v.v.}} \sim -1.55 \times 10^{-4}$ [emu/mol f.u.], and the saturated value of $\chi_{\text{spin}} \sim 4.77 \times 10^{-4}$ [emu/mol f.u.] below 50 K. Using $N(E_f) = 4.99$ [states/eV f.u.] [15] implies that the enhancement of the spin susceptibility χ_{spin} over the band value $\chi_{\text{band}} = 1.61 \times 10^{-4}$ [emu/mol f.u.] is $\chi_{\text{spin}}/\chi_{\text{band}} \sim 3.0$. This is to be compared with the specific heat enhancement $\gamma/\gamma_{\text{band}} \sim 2.6$ [15]. These estimations give the Wilson ratio $R_W = \frac{\chi_{\text{spin}}/\chi_{\text{band}}}{\gamma/\gamma_{\text{band}}} \sim 1.15$ (see also [8]). $R_W = 2$ is expected in the strongly correlated limit, while $R_W = 1$ in the uncorrelated case, therefore $R_W = 1.15$ indicates that the electrons are in a mildly correlated state.

In Fig. 2(b), we present the temperature dependence of the ^{13}C nuclear spin-lattice relaxation rate $1/^{13}T_1$ divided by temperature T , $1/^{13}T_1T$. Figure 1(b) is an example of nuclear spin recovery after saturation. Theoretically, the spin contribution to $1/^{13}T_1T$ may be written as the wave vector \mathbf{q} summation of the imaginary part of the dynamical electron spin susceptibility $\chi''(\mathbf{q}, \omega_n)$,

$$\frac{1}{T_1T} = \frac{\gamma_n^2 k_B}{\mu_B^2 \hbar} \sum_{i,j} \sum_{\mathbf{q}} |A_{ij}(\mathbf{q})|^2 \frac{\chi''_{i,j}(\mathbf{q}, \omega_n)}{\omega_n}, \quad (2)$$

where $\gamma_n = 10.7054$ MHz/T is the nuclear gyromagnetic ratio of ^{13}C , ω_n is the resonance frequency, and i, j are band indices [17,19,20]. As emphasized earlier by Walstedt and Cheong [20], cross terms between different bands can exist for the spin-lattice relaxation process, while such cross terms do not exist in NMR Knight shifts [17]. This makes separation of various contributions to $1/T_1T$ a nontrivial matter in multiband systems such as MgCNi_3 and Sr_2RuO_4 .

The most striking aspect of the $1/^{13}T_1T$ data is the continuous increase of its magnitude all the way from 800 to about 20 K through $T^* \sim 50$ K. Our results indicate that spin fluctuations are nearly a factor 3 enhanced with decreasing temperature. Within a simple Fermi-liquid picture ignoring all the complications from the multiband effects mentioned above (i.e., we assume that the two sets of d - p bands exhibit identical temperature dependences of the spin susceptibility), a modified Korringa law, $1/T_{1,\text{spin}}TK_{\text{spin}}^2 = 1/S\beta$, should hold [19,21]. Here

$1/T_{1,\text{spin}}$ and K_{spin} are the spin contributions, and $S = (\frac{\hbar}{4\pi k_B})(\frac{\gamma_c}{\gamma_n})^2 = 4.17 \times 10^{-6} \text{ sec K}$ for ^{13}C . β is a quantity that signifies the effects of electronic correlations. In this scenario, the observed 50% to 70% increase in the spin contribution to the Knight shift ^{13}K between 800 and 120 K implies that $1/^{13}T_1T$ would also increase by a factor $1.5^2(= 2.3)$ to $1.7^2(= 2.9)$ by the Korringa process from electron-hole pair excitations at the Fermi level. This is consistent with the factor 2.6 increase of $1/^{13}T_1T$ in the same temperature range. In fact, as shown in the inset to Fig. 2(a), above 120 K we can fit $1/^{13}T_1T$ and ^{13}K to the modified Korringa relation $1/^{13}T_1T = 1/^{13}T_{1,\text{orb}}T + (^{13}K - ^{13}K_{\text{orb}})^2/S\beta$ with $\beta = 6.0$, the orbital contribution $1/^{13}T_{1,\text{orb}}T = 0.005 \text{ sec}^{-1}\text{K}^{-1}$, and $^{13}K_{\text{orb}} = 0.014\%$. When one is dealing with correlation effects in a three-dimensional electron gas with a spherical Fermi surface, $\beta = 1$ for the uncorrelated case, and $\beta > 1$ for the ferromagnetically correlated case. On the other hand, the enhancement of low frequency spin fluctuations at nonzero wave vectors affects only $1/T_1T$, and hence tends to reduce β . The successful fit of $1/^{13}T_1T$ and ^{13}K by a modified Korringa law with $\beta = 6.0$ suggests that above 120 K the d - p bands in MgCNi_3 form a Fermi-liquid state with relatively strong ferromagnetic correlation effects. This is consistent with the strong enhancement of the uniform spin susceptibility with decreasing temperature. We must caution, however, that $\beta = 6.0$ may be somewhat too large due to the fact that we have ignored the presence of two bands that would tend to overestimate β by a factor ~ 2 [17]. Furthermore, as noted by Moriya [19], the precise magnitude of β is sensitive to the deviation of the Fermi surface from spherical symmetry. We call for more sophisticated band theoretical analysis of our data to clarify the nature of the correlation effects at the quantitative level.

Even though the modified Korringa law describes our data reasonably well above 120 K, it is important to notice that a single modified Korringa relation cannot account for the continuous increase of $1/^{13}T_1T$ below 120 K through $T^* \sim 50$ K down to ~ 20 K. In this regime, ^{13}K shows a crossover to a low temperature constant regime. The fact that the overall spin fluctuations reflected in the wave vector integral of $\chi''(\mathbf{q}, \omega_n)$ increase while the $\mathbf{q} = \mathbf{0}$ component of the total static spin susceptibility $\sum_j \chi'_j(q = 0)$ maintains a constant magnitude strongly suggests that spin fluctuations with finite wave vectors away from $\mathbf{q} = \mathbf{0}$ continue to grow significantly below $T^* \sim 50$ K. In this context, it is important to realize that band calculations suggest the presence of strong nesting effects between some segments of the Fermi surface [14,15]. If the nesting effects are indeed substantial, spin fluctuations corresponding to the nesting wave vectors could indeed continue to grow below $T^* \sim 50$ K.

Both ^{13}K and $1/^{13}T_1T$ are saturated below 20 K. Using the same orbital contributions as before, the modified Korringa relation for the correlated Fermi liquid gives

$\beta = 4.7$ below 20 K. This value is smaller than $\beta = 6.0$ observed above 120 K by 20%, again signaling the importance below 20 K of correlation effects with finite wave vectors. Putting all the pieces together, we obtain the following physical picture for the normal state of MgCNi_3 : the electrons in the Ni-C d - p bands are modestly correlated; the primary channel of the correlation effects appears to be centered near $\mathbf{q} = \mathbf{0}$ above 50 K but spin fluctuations with finite wave vectors $\mathbf{q} \neq \mathbf{0}$ show continuous growth down to 20 K, below which electron correlation effects are saturated with $R_W = 1.15$. Extensive efforts are underway to understand the electronic properties of MgCNi_3 based on band calculations [13–16], and our experimental data provides a good testing ground for those theories. It is worthwhile recalling that a similar situation is also encountered in Sr_2RuO_4 . The ^{17}O NMR Knight shifts in Sr_2RuO_4 increase with decreasing temperature and even begin to decrease below $T^* \sim 50$ K. On the other hand, $1/^{17}T_1T$ continues to grow through 50 K [4]. Subsequent inelastic neutron scattering measurements revealed that an anomalous enhancement of spin fluctuations corresponding to the nesting vectors of quasi-one-dimensional $4d_{yz,zx}$ bands is responsible for the continuous increase of $1/^{17}T_1T$ towards T_c [5].

Next, we turn our attention to the behavior of $1/^{13}T_1$ in the superconducting state. As shown in Fig. 3(a), a magnetic field of 9 T destroys superconductivity down to ~ 2.5 K, above which $1/^{13}T_1$ maintains a Korringa behavior $1/^{13}T_1T = 0.072 \text{ sec}^{-1}\text{K}^{-1}$. However, at lower magnetic fields, $1/^{13}T_1$ is enhanced just below T_c , peaks at $\sim 0.9T_c(H)$, and is followed by an exponential decrease at lower temperatures. Moreover, the peak value of $1/^{13}T_1$ just below T_c grows with decreasing magnetic field from 1 to 0.45 T. For the lowest field at $H = 0.45$ T, $1/^{13}T_1$ is

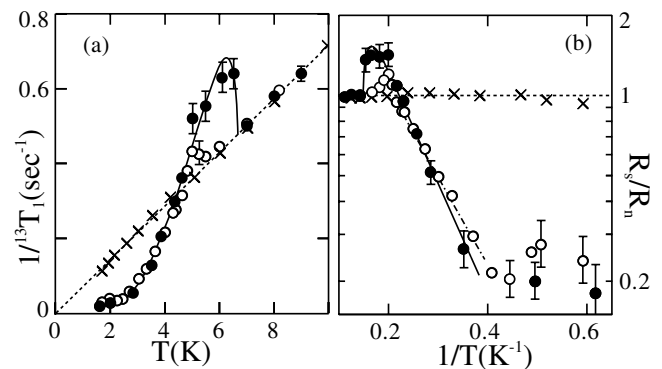


FIG. 3. (a) $1/^{13}T_1$ measured at 0.45 T (\bullet), 1 T (\circ), and 9 T (\times). The dashed line represents $1/^{13}T_1T = 0.072 \text{ sec}^{-1}\text{K}^{-1}$. The solid line through 0.45 T data is the standard BCS fit with mean gap magnitude $\langle \Delta(H = 0.45 \text{ T}) \rangle / k_B \sim 10.5$ K and mean square anisotropy $\langle a^2(\mathbf{\Omega}) \rangle \sim 0.047$ (see text). (b) The same data and lines as (a) plotted as $R_s = 1/^{13}T_1T$ divided by $R_n = 0.072 \text{ sec}^{-1}\text{K}^{-1}$ on a semilogarithmic scale as a function of inverse temperature $1/T$. The dash-dotted line through 1 T data is a fit in the low temperature region to $e^{-(\Delta(H=1 \text{ T})) / k_B T}$ with $\langle \Delta(H = 1 \text{ T}) \rangle / k_B \sim 8$ K.

enhanced by a factor ~ 1.4 just below $T_c(H = 0.45 \text{ T}) = 6.7 \text{ K}$. A similar robust enhancement is usually observed in conventional BCS superconductors due to the pileup of the density of quasiparticle excitations, and is known as the Hebel-Slichter coherence peak [22,23]. The temperature dependence of the coherence peak can be fit by incorporating a minor \mathbf{k} -space anisotropy in the conventional s -wave gap [23]

$$\Delta(H, \mathbf{\Omega}) = \langle \Delta(H) \rangle [1 + a(\mathbf{\Omega})], \quad (3)$$

where $\mathbf{\Omega}$ is the solid angle in \mathbf{k} space, $\langle \Delta(H) \rangle$ is the mean gap value over all orientations in \mathbf{k} space, and $a(\mathbf{\Omega})$ is the small anisotropy function satisfying the condition $\langle a(\mathbf{\Omega}) \rangle = 0$. The best fit results, shown in Fig. 3, yield a mean gap magnitude of $\langle \Delta(H = 0.45 \text{ T}) \rangle / k_B \sim 10.5 \text{ K}$ and mean square anisotropy $\langle a^2(\mathbf{\Omega}) \rangle \sim 0.047$ in a magnetic field of 0.45 T, or equivalently $\frac{\langle \Delta(H) \rangle}{k_B T_c(H)} \sim 1.6$ which is consistent with the standard BCS value of $\frac{\langle \Delta(H=0) \rangle}{k_B T_c(H=0)} = 1.75$ [24]. $\langle \Delta(H) \rangle$ may be somewhat underestimated by the influence of H since $\langle \Delta(H = 1 \text{ T}) \rangle$ is smaller than $\langle \Delta(H = 0.45 \text{ T}) \rangle$, as shown in Fig. 3(b).

We also noticed that the exponential decrease of $1/^{13}\text{T}_1$ saturates below $\sim 2.5 \text{ K}$ and that the magnitude of $1/^{13}\text{T}_1$ itself is distributed below this temperature. It is known [18] that a large “flux avalanche” effect occurs below 3 K in MgCNi_3 , and the saturation of $1/^{13}\text{T}_1$ is most likely due to the fluxoid contribution [23,25,26]. Unfortunately, the fluxoid effects prevented us from confirming the exponential decrease in $1/^{13}\text{T}_1$ down to the lowest temperature. We should caution that, theoretically, a small peak in $1/^{13}\text{T}_1$ is known to arise even in non- s orbital pairing symmetries as long as singularities exist in the quasiparticle excitation spectrum. However, we are not aware of any materials with anisotropic pairing symmetry that shows such a robust coherence peak with the appropriate magnetic field dependence.

Given the qualitative similarities of the normal state NMR data between MgCNi_3 and the unconventional superconductor Sr_2RuO_4 [3], the possible realization of conventional s -wave symmetry superconductivity in the former may be rather surprising. However, we point out that correlation effects in the three-dimensional material MgCNi_3 are expected to be much weaker than in the quasi-two-dimensional material Sr_2RuO_4 [14,15]. Furthermore, the presence of the light C atom in the structure might create high frequency phonons and help open the s -wave channel at a higher temperature than the p - or d -wave channels.

In fact, $T_c = 7 \text{ K}$ of MgCNi_3 is several times higher than $T_c = 1.4 \text{ K}$ of Sr_2RuO_4 .

To summarize, we have reported the first ^{13}C NMR measurements in MgCNi_3 . The strong temperature dependence of ^{13}K and $1/^{13}\text{T}_1T$ and subsequent saturation below ~ 50 and $\sim 20 \text{ K}$, respectively, are consistent with the presence of modest electronic correlation effects, possibly assisted by nesting effects. This suggests that the electronic state has reached a modestly mass-enhanced Fermi-liquidlike state prior to the superconducting transition. The robust coherence peak and subsequent exponential decrease of $1/^{13}\text{T}_1$ is consistent with s -wave pairing.

The work at MIT was supported by NSF DMR 98-08941 and 99-71264, and at Princeton by NSF DMR 97-25979 and DOE DE-FG02-98-ER45706.

-
- [1] N. D. Mathur *et al.*, Nature (London) **394**, 39 (1998).
 - [2] Y. Maeno *et al.*, Nature (London) **372**, 532 (1994).
 - [3] K. Ishida *et al.*, Phys. Rev. B **56**, R505 (1997).
 - [4] T. Imai *et al.*, Phys. Rev. Lett. **81**, 3006 (1998).
 - [5] Y. Sidis *et al.*, Phys. Rev. Lett. **83**, 3320 (1999).
 - [6] I. Nagamatsu *et al.*, Nature (London) **410**, 63 (2001).
 - [7] T. He *et al.*, Nature (London) **411**, 54 (2001).
 - [8] M. A. Hayward *et al.*, Solid State Commun. **119**, 491 (2001).
 - [9] S. Y. Li *et al.*, Phys. Rev. B **64**, 132505 (2001).
 - [10] Q. Huang *et al.*, cond-mat/0105240.
 - [11] Z. Q. Mao *et al.*, cond-mat/0105280.
 - [12] Z. A. Ren *et al.*, cond-mat/0105366.
 - [13] S. B. Dugdale *et al.*, Phys. Rev. B **64**, 100508 (2001).
 - [14] J. H. Shim and B. I. Min, cond-mat/0105418.
 - [15] D. J. Singh *et al.*, Phys. Rev. B **64**, 140507 (2001).
 - [16] H. Rosner *et al.*, cond-mat/0106583.
 - [17] Y. Yafet and V. Jaccarino, Phys. Rev. **133**, A1630 (1964).
 - [18] N. P. Ong (private communication).
 - [19] T. Moriya, J. Phys. Soc. Jpn. **18**, 516 (1963).
 - [20] R. E. Walstedt and S.-W. Cheong, Phys. Rev. Lett. **72**, 3610 (1994).
 - [21] A. Narath and H. T. Weaver, Phys. Rev. **175**, 373 (1968).
 - [22] L. C. Hebel and C. P. Slichter, Phys. Rev. **113**, 1504 (1959).
 - [23] D. E. MacLaughlin, Solid State Phys. **31**, 1 (1976).
 - [24] Another conventional NMR approach to clarify the pairing symmetry of the superconducting state is to measure the Knight shift below T_c . Unfortunately, we found that the resonance linewidth becomes even broader than the magnitude of the normal state Knight shift due to fluxoid effects [see Fig. 1(a)].
 - [25] S. M. De Soto *et al.*, Phys. Rev. Lett. **70**, 2956 (1993).
 - [26] V. A. Stenger *et al.*, Phys. Rev. Lett. **74**, 1649 (1995).